Distributed Brillouin fiber optic temperature sensing for hydrogeology

Maxime Romanet, Jordan Labbe, Alexandre Matic, Maxime Zerbib, Philippe Amiotte- Suchet, Xavier Bertrand, Thomas Karbowiak, Kien Phan Huy, Hélène Celle, and Jean-Charles Beugnot,

***Abstract*— In this paper, we demonstrate application of Brillouin-based distributed fiber optic sensors for hydrogeology, conducted at an experimental site located at Port Douvot, near the city of Besançon in East of France. The flow measurement is achieved using an active heating method and distributed fiber sensor instrument with spatial resolution of 1 meter, a temperature resolution of 0.2 °C, and an acquisition time of 1 min 30s. Brillouin-based instruments offer the advantage of frequency-dependent temperature measurements, simplifying the system setup.**

***Index Terms*— Stimulated Brillouin scattering, optical fiber, distributed temperature fiber measurement, active heating distributed fiber sensor, groundwater flow measurement.**

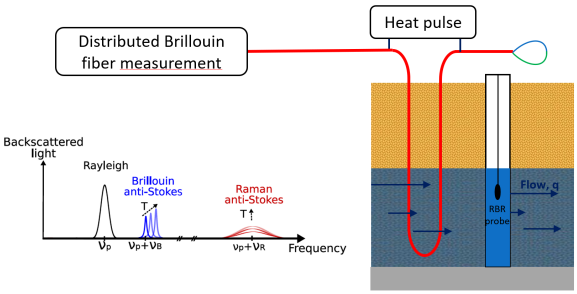

I. Introduction

Aquifer heterogeneity plays a crucial role in governing the movement of water and the transport of contaminants, which are fundamental processes in managing and mitigating contamination [1]. The variability in an aquifer's properties, such as hydraulic conductivity and porosity, significantly influences pollutants spread. The hydrodynamic properties, as hydraulic conductivity K, can vary by several orders of magnitude over just a few meters [2], [3]. Each hydrofacies can therefore be characterized by its own hydraulic conductivity [4]. Highly connected, coarse-grained hydrofacies (cobbles, gravels) characterized by spatial continuity allow the formation of preferential flow paths and can thus promote rapid advective transport [5]. We therefore understand that heterogeneity directly impacts the transport of various particles/solutes/contaminants [6]–[8] and that its characterization is necessary for environmental engineering operations such as defining protection zones for drinking water wells or implementing effective remediation strategies for contaminated sites [9]. Distributed fiber sensors, utilizing light scattering, can monitor strain, temperature, and vibration along optical fiber cables [10], [11]. The three primary types of scattering—Rayleigh, Brillouin, and Raman—enable precise distributed temperature measurements as represented on fig 1. The light scattering spectrum in optical fibers is influenced by temperature, affecting both the amplitude and frequency of the light scattering.

In recent years, distributed temperature and vibrations fiber sensors have been increasingly utilized in geological applications [12]–[14] and new applications include leak detection in hydrogen energy storage [15]. Rayleigh scattering-based instruments can measure temperature variations with a precision of less than 0.1 °C and a spatial resolution of 1 cm. However, these measurements are highly sensitive to environmental fluctuations and require frequent calibration [16]. Some applications require long-term monitoring as soil moisture observations [17] and temperature events detections in industrial applications [18]. Raman scattering, where temperature variations impact the intensity of Stokes and anti-Stokes component, commonly used in hydrogeology, can provide measurements in few second with a spatial resolution of 0.3 m and temperature sensitivity of 0.1°C, though it also needs continuous calibration [19], [20]. These systems are easy to implement but necessitate continuous calibration throughout the measurement process [21], which introduces uncertainty in the temperature readings. In contrast, Brillouin scattering-based instruments provide temperature and strain measurements in frequency domain, unlike Rayleigh and Raman systems. In geology, Brillouin scattering was classically used to monitor the strain on land-shape and soil slopes [22], [23]. They can operate with standard telecommunication fibers and offer a spatial resolution and sensitivity of 0.5 m and 0.2 °C, respectively, which is closed to Raman systems.

This work was supported by the ISITE-BFC (Initiatives Science Innovation Territoire Economie en Bourgogne-Franche-Comté) through the SENSAAS (SENSors and Analyses for AquiferS) ISITE-BFC project (grant number: FC21010.CHR.IS - SENSAAS), EIPHI Graduate school (contract "ANR-17-EURE-0002") and TRANSBIO Graduate school.

M. Romanet, A. Matic, M. Zerbib and J-C. Beugnot are with the Université Marie et Louis Pasteur, Institut FEMTO-ST, CNRS, Besançon, France (e-mail: jc.beugnot@femto-st.fr).

J. Labbe, H. Celle are with the Université Marie et Louis Pasteur, Chrono-Environnement, CNRS, Besançon, France.

P. Amiotte-Suchet is with the Université Bourgogne Europe, CNRS, Biogéosciences, Dijon, France.

X. Bertrand is with the Hygiène Hospitalière, Centre Hospitalier Universitaire de Besançon, Besançon, France.

T. Karbowiak is with the Institut Agro Dijon, PAM, Dijon, France.

K. Phan Huy is with the SUPMICROTECH-ENSMM, 16 rue de l'épitaphe, Besançon, France.

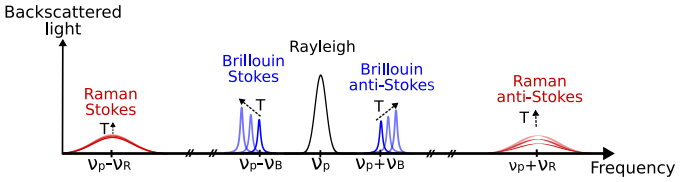

Fig. 1. Backscattering light spectrum in silica optical fiber with the effect of temperature variation on amplitude and frequency of the light scattering.

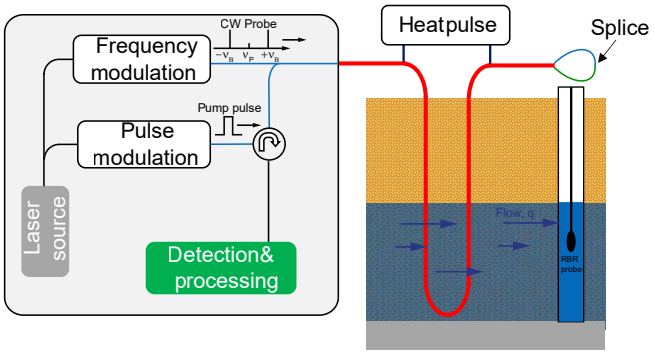

Fig. 2. Technical configuration for pump/probe Brillouin measurement (BOTDA) for distributed temperature measurement along an optical cable. A pulsed light source is launched into an optical fiber, and an optical signal, frequency-shifted relative to the Brillouin frequency, is launched in the opposite direction. The amplified signal is detected with a photodiode, and the Brillouin shift is obtained through post-processing.

More generally, to monitor the temperature and the strain along range close to 100 km, during several weeks (without calibration) Brillouin scattering technology can be a reliable solution. Advancements in optoelectronic devices have significantly enhanced measurement capabilities, enabling industrial equipment to complete analyses within just one minute.

In hydrogeology, heat serves as an effective tracer for characterizing the spatial distribution of groundwater fluxes [24]. Among the methods leveraging thermal tracing, Thermal Response Tests (TRTs), first introduced by [25], provide an in situ approach for evaluating subsurface thermal conductivity and borehole thermal resistance. TRTs rely on a one-dimensional conductive heat transfer model to describe the mean temperature increase at a radial distance from an infinite heat source with constant heat flux, assuming a fixed boundary temperature at an infinite radial distance. In conventional TRTs, a high-power source (50–80 W/m) heats water circulating within a ground heat exchanger (GHE), producing a temperature differential of 3–7 °C between the GHE inlet and outlet. This setup simulates geothermal system operation, while the estimated bulk thermal conductivity reflects an average value along the borehole. However, this estimate can be influenced by subsurface heterogeneity and groundwater flow, which may introduce variability in thermal properties. To address these challenges, fiber optic distributed temperature sensing (FO-DTS) enables high-resolution temperature profiling during TRTs, offering a refined approach for assessing vertical variations in thermal conductivity and subsurface heterogeneity. A novel approach for measuring groundwater flow has been demonstrated through the integration of a distributed temperature fiber optic sensor with a heat pulse system [26]–[28]. Complementing this, active distributed temperature sensing (A-DTS) has become widely deployed for hydrogeological measurements, particularly in deep wells, where it provides significant advantages over traditional point-based methods. [27], [29], [30]. This innovative method allows for high-resolution, real-time monitoring of subsurface water movement, improving accuracy and efficiency in groundwater studies.

In this study, we aim to validate Brillouin optical fiber sensor technology by precisely measuring temperature differences. This is achieved through the continuous and uniform heating of the optical fiber cable while simultaneously monitoring the background temperature of the groundwater system. Additionally, this method enables the quantification of vertical thermal conductivity, offering a reliable and advanced technique for hydrogeological studies. These findings contribute to improved groundwater monitoring and management strategies.

II. Principle of Distributed Brillouin Fiber Measurement

The distributed sensing method, known as Brillouin Optical Time Domain Analysis (BOTDA), is illustrated in Figure 2. A single laser source, a DFB laser operating at a telecommunication wavelength (ν_P), was used to generate both pump and probe waves. The pump pulses (green line) were generated by optical modulation and then amplified using an erbium-doped fiber amplifier to achieve power levels of several hundred milliwatts. These amplified pump pulses were then directed into the optical fiber cable via an optical circulator, propagating in the opposite direction to the continuous wave probe signal to induce local Brillouin amplification. The probe signal was modulated using an electro-optic modulator to produce two different modulation frequencies corresponding to the Brillouin Stokes ($-\nu_B$) and anti-Stokes (ν_B) shifts. The amplified probe signal was detected using a photodiode. The frequency difference between the pump and probe was scanned around ν_B, and the frequency of amplified probe signal was recorded at each point along the fiber. The spatial resolution is determined by the duration of the pump pulse. In 2006, the first demonstration of temperature measurement along an optical fiber using Brillouin scattering showcased the potential of this technology for geological applications [31]. However, Brillouin-based temperature measurements typically require several minutes to map the temperature along the optical fiber due to frequency scan.

III. Experimental Configuration

The experimental site is located in the floodplain of the Doubs river as depicted in Figure 3. The alluvial plain consists of recent alluvial deposits of calcareous nature, laid down by the Doubs, which flows from the north-east to the south-west through an environment characterized by limestone hills typical of this geological area. Port-Douvot is situated on

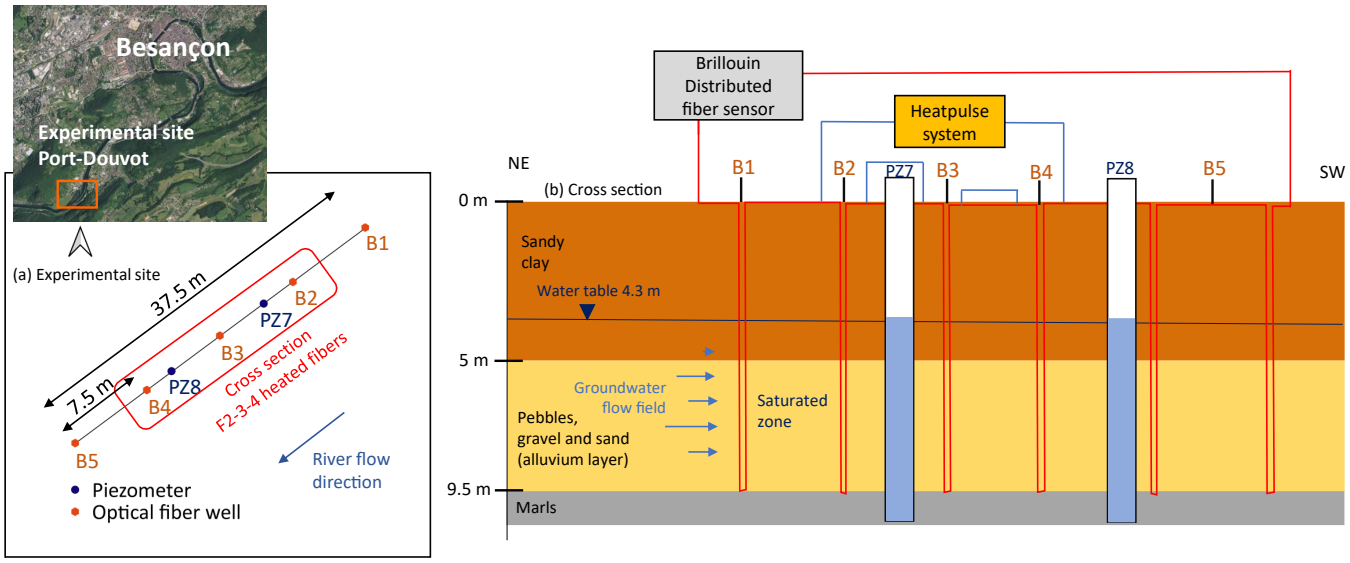

Fig. 3. Schematic of active distributed temperature measurement principle based on Brillouin backscattering detection (BOTDA). The experimental environment site of Port Douvot close to Besançon city is represented. The heat pump system is connected to only three borehole (B2, B3, B4). The first (B1) and last (B5) boreholes are used as reference. An electrical sampling of 0.25 cm with an optical spatial resolution of 1 m are used for measurement.

the right bank of the river, where the lateral extent of the alluvial aquifer is 160 m. The alluvial deposits are composed of sandy-gravelly sediments and may be locally overlain by low-permeability silty sediments [32]. The alluvial aquifer upstream of the site is characterized by a hydraulic conductivity ranging from $10^{-}2$ m/s to $10^{-}4$ m/s and a storage coefficient between 0.01 to 0.03, which are characteristic of an unconfined aquifer [33]. Piezometric data from boreholes BSS001JHAY and BSS001JHAZ (Figure III. 3, https://ades.eaufrance.fr/) indicate altitudinal variations in the water table ranging from 232.37 m NGF (low water level) to 235.85 m NGF (high water level). The alluvial aquifer flows parallel to the Doubs, from the north-east to the south-west.

A commercial distributed temperature sensing device (DITEST) is employed to measure temperature along the optical fiber cable [34]. A splice between the two SMF is realized at the end of cable to used the pump/probe configuration (BOTDA). Along 37.5 m, an optical fiber cable is installed on ground flow parallel to the river. We used an industrial cable (diameter 4.8 mm) with 6 optical fibers (4 multimode fibers and 2 single mode fibers) on the loose tube to remove strain effect and detect only temperature variation. The boreholes were drilled by a specialized company, and the fiber optic cable was installed and manually weighted to achieve a U-shaped configuration. Following installation in all five boreholes, the fiber optic cables were spliced together to form a continuous fiber loop. The measurement campaign was conducted several months after installation to allow the boreholes to naturally seal, thereby ensuring stable and representative conditions for data acquisition. The steel armed protection is used to heat different section of the cable on borehole (B2, B3, B4). The different piezometer close to the borehole (Noted PZX on Figure3) store the temperature every minute with a precision of 0.01 °C.

The BOTDA-type instrument performs a frequency sweep to measure the Brillouin backscattering spectrum, which then gives access to an absolute temperature variation after calibration processs. The temperature Brillouin coefficient in single mode fiber with laser emitting at 1550 nm is equal to 1.07 MHz/°C [10], [35]. Thanks to this dependence, and by measuring the frequency of the Brillouin backscattering along the optical fiber, we can deduce the temperature along the infrastructure. The frequency scan will be centered around the Brillouin response of the optical fiber used. In our case, the frequency scan is carried out from 10.7 GHz to 11 GHz with a step of 1 MHz, with an averaging of 5600 on each frequency, in order to get the best frequency measurement.

To facilitate groundwater flow measurement, a thermal anomaly along the optical fiber is necessary. We employed an electrical heating technique to uniformly heat the cable throughout the borehole. This uniform heating along the borehole length can be achieved through Joule heating in an electrical conductor. The same cable used for Distributed Temperature Sensing (DTS) can be directly heated by passing electrical currents through its metallic armoring, provided that an electrical connection is established at both ends of the cable [36].

IV. Data and Results

The SMF is spliced at the end of the cable to realize easily the BOTDA configuration. A time interval of 1min30s between two measurements was deemed optimal to obtain both sufficient temporal sampling and a sufficiently accurate temperature measurement. The smaller the frequency sampling, the better the temperature resolution. Spatial resolution was set at 1 m (10 ns optical pulses), which is the smallest spatial resolution possible with our instrument, with one measurement point every 25 cm. As the optical

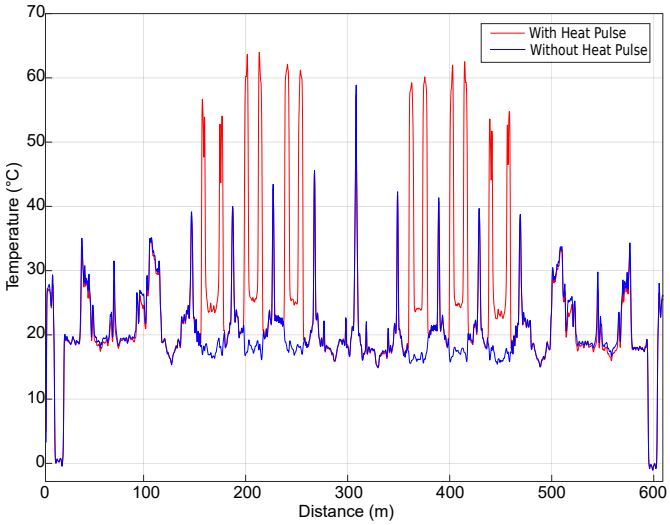

Fig. 4. Distributed temperature profiles recorded with the Ditest instrument all along the SMF in BOTDA configuration with 1 m spatial resolution, 0.25 m sampling and 1min30s acquisition time. The blue and red line present the measurement without and with heat pulse, respectively.

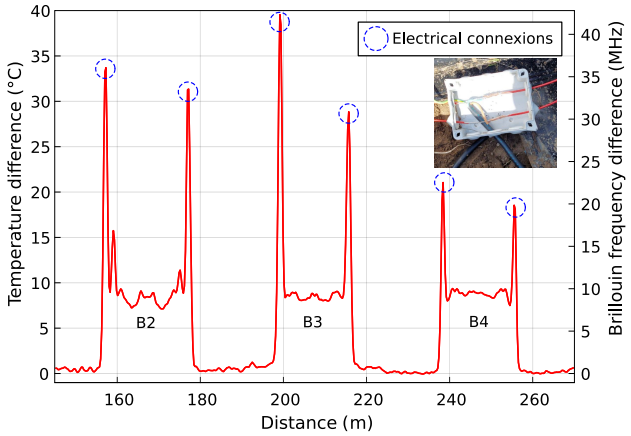

Fig. 5. Distributed measurement with the BOTDA configuration along the optical fiber cable centered to the three heated boreholes. The temperature shown corresponds to the difference between the measurement at 45 minutes, and the measurement at time equal to zero in degrees (℃). On the right axis, we show the original Brillouin frequency difference in MHz. The temperature coefficient for single mode fiber at the wavelength of 1550 nm is 1.07 MHz/℃. caption represents a picture of electrical connection with optical cable armored.

fiber range measurement is shorter than 500 m, the laser repetition rate was increased to 25 kHz. In order to heat the cable and the environment, a heat pump system is used with a launched power of 9 W/m. The Brillouin spectrum has a Lorentzian spectral distribution and a quadratic least-square fitting was used to extract the Brillouin frequency. From the frequency profile, and thanks to the coefficient temperature, the distributed temperature measurement in single mode fiber along the optical cable is represented in figure 4. Measurement in stainless loose-tube confirmed temperature measurement itself. The thermal expansion of optical fiber cable is neglected because the maximum temperature variation during measurement is less than 10°C. The blue line shows the temperature evolution at one moment during the day. The symmetry of the temperature profile centered at 305 m is due to the splice end for BOTDA configuration. The red line represents the temperature along the fiber after some minutes of heating by heat pulse. The three boreholes (B2, B3, B4) heated simultaneously with the heat pulse are clearly visible.

A zoom on heated fiber on 3 boreholes are represented in Figure 5. Boreholes are located between 158 m and 178 m (Borehole 2), between 195 and 215 m (Borehole 3), and between 235 m and 255 m for the borehole 4 (B4). On the different boreholes, the temperature difference due to the heated system at the bottom of the borehole is around 9°C. On each side of the boreholes, we observe temperature peaks due to electrical connections, which are circled in blue. The high temperature up to 60°C at electrical connections due to materials difference between electrical cable and optical cable armored (copper vs steel) makes the first few meters of fiber unusable. Only the bottom 5 meters of the well are usable, since they correspond to the 5 meters of the saturated zone of the aquifer, hence the zone where flux measurement is possible. Above the 5 meters, the fiber is in contact with air,

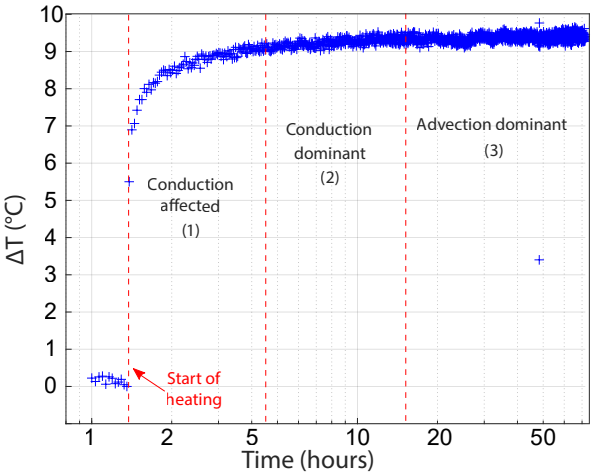

Fig. 6. Temperature measurement at the bottom of the borehole 3 during a heating of 72 hours with a power of 9 W/m. Each point is the average between 5 consecutive points in time. The sampling interval is 0.25 m and the spatial resolution is 1 m.

sand, and gravel. Active distributed fiber sensor method cannot be used for the few meters of optical fiber around the electrical connection because the thermal change induced by joule effect is very large.

1) Temperature measurements: Heat transfer with convection, conduction, and advection through the porous media are clearly visible on figure 6. Experimental thermal response curves (Figure 6) reveal three distinct phases: (1) an initial, rapid temperature rise independent of flow conditions; (2) conduction-dominated heat transfer, modulated by groundwater flow; and (3) advection-dominated heat transfer. These observations are consistent with theoretical and experimental advancements in heat transfer mechanisms, as documented in recent studies [19], [37]–[39]. The steady state is reached when

the flow of cold groundwater compensates for the heat input of the heat pulse.

2) Thermal conductivity measurements: We use the conduction-dominated phase to determine the distribution of thermal conductivities λ (W/m/K) along the FO cables in boreholes 2, 3, and 4. The hydrogeology measurement are describes in this work [40].

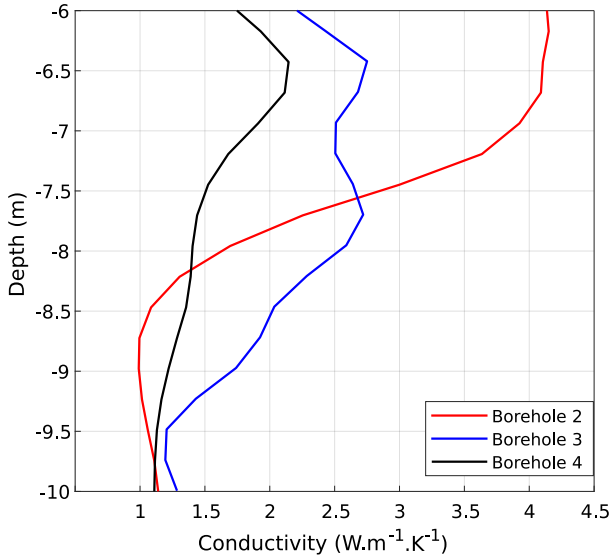

Fig. 7. Experimental measurement of thermal conductivity as a function of distance, for the different boreholes studied.

The figure 7 shows the thermal conductivity measured along the boreholes 2, 3 and 4. To improve accuracy, we plot the average value between the downward and upward measurements, as both record conductivity at the same depth level. The depth in the wells is shown on the y-axis, while thermal conductivity is on the x-axis. Only the submerged section (in contact with groundwater) is displayed to ensure physically meaningful values. Outside these zones, the experiment is not feasible due to the absence of water flow around the cable (unsaturated zone of the aquifer). The conductivity difference is mainly due to the inhomogeneity of the medium [41]. These measurements are in good agreement with thermal conductivity values reported in the literature for alluvial deposits range from 1.17 to 3 W/m/K [42]–[44].

V. Conclusion

We successfully demonstrated the use of an active distributed temperature fiber sensor based on the Brillouin scattering process for characterizing groundwater flow at an experimental site. The BOTDA configuration in single mode fiber achieved a spatial resolution of 1 meters and an acquisition time of 1 minute and 30 seconds, with a temperature measurement uncertainty of 0.2°C. Our findings indicate that Brillouin scattering-based temperature sensors in loosely-tubed single-mode fiber are well-suited for hydrogeological applications. However, A key advantage of this approach is the ability to perform frequency-dependent temperature measurements, making it particularly valuable for long-term monitoring without the need for frequent calibration. Future work will focus on a comparative study between Brillouin and Raman sensors at the same experimental site to evaluate their respective performance in groundwater monitoring. The advancement of faster measurement techniques [45], [46], including Brillouin measurement in multimode fiber [47], along with high-resolution and high-sensitivity capabilities, opens new possibilities for hybrid Raman-Brillouin measurements applied to geological and hydrogeological studies.

Acknowledgment

We thank Olivier Bour from Geosciences Rennes for fruitful discussions and helping us during the experimental work.

References

[1] J. R. Allen, "A review of the origin and characteristics of recent alluvial sediments," *Sedimentology*, vol. 5, no. 2, pp. 89–191, 1965.
[2] S. Boggs Jr, *Petrology of sedimentary rocks*. Cambridge university press, 2009.
[3] C. E. Koltermann and S. M. Gorelick, "Heterogeneity in sedimentary deposits: A review of structure-imitating, process-imitating, and descriptive approaches," *Water Resources Research*, vol. 32, no. 9, pp. 2617–2658, 1996.
[4] G. S. Weissmann, Y. Zhang, E. M. LaBolle, and G. E. Fogg, "Dispersion of groundwater age in an alluvial aquifer system," *Water Resources Research*, vol. 38, no. 10, pp. 16–1, 2002.
[5] M. Bianchi and C. Zheng, "A lithofacies approach for modeling non-f ickian solute transport in a heterogeneous alluvial aquifer," *Water Resources Research*, vol. 52, no. 1, pp. 552–565, 2016.
[6] R. F. Anderson, S. L. Schiff, and R. H. Hesslein, "Determining sediment accumulation and mixing rates using 210pb, 137cs, and other tracers: problems due to postdepositional mobility or coring artifacts," *Canadian Journal of Fisheries and Aquatic Sciences*, vol. 44, no. S1, pp. s231–s250, 1987.
[7] D. S. Sinton, J. A. Jones, J. L. Ohmann, and F. J. Swanson, "Windthrow disturbance, forest composition, and structure in the bull run basin, oregon," *Ecology*, vol. 81, no. 9, pp. 2539–2556, 2000.
[8] T. S. Sarris, M. Close, and P. Abraham, "Using solute and heat tracers for aquifer characterization in a strongly heterogeneous alluvial aquifer," *Journal of hydrology*, vol. 558, pp. 55–71, 2018.
[9] N. Gueting, A. Klotzsche, J. van der Kruk, J. Vanderborght, H. Vereecken, and A. Englert, "Imaging and characterization of facies heterogeneity in an alluvial aquifer using gpr full-waveform inversion and cone penetration tests," *Journal of hydrology*, vol. 524, pp. 680–695, 2015.
[10] A. H. Hartog, *An Introduction to Distributed Optical Fibre Sensors*. CRC Press, 2017.
[11] G. Bolognini and A. Hartog, "Raman-based fibre sensors: Trends and applications," *Optical Fiber Technology*, vol. 19, no. 6, pp. 678–688, 2013.
[12] M. Shanafield, E. W. Banks, J. W. Arkwright, and M. B. Hausner, "Fiber-Optic Sensing for Environmental Applications: Where We Have Come From and What Is Possible," *Water Resources Research*, vol. 54, no. 11, pp. 8552–8557, 2018. [Online]. Available: https://onlinelibrary.wiley.com/doi/10.1029/2018WR022768
[13] L. Schenato, "A Review of Distributed Fibre Optic Sensors for Geo-Hydrological Applications," *Applied Sciences*, vol. 7, no. 9, p. 896, 2017. [Online]. Available: http://www.mdpi.com/2076-3417/7/9/896
[14] M. Liu, L. Costa, P. Mertz, S. Varughese, S. Edirisinghe, V. Kamalov, and Z. Zhan, "Trans-oceanic distributed sensing of tides over telecommunication cable between portugal and brazil," *Geophysical Research Letters*, vol. 52, no. 12, p. e2024GL114414, 2025.
[15] E. Dejband, T.-H. Tan, Y. C. Manie, C.-K. Yao, T.-C. Lin, H.-M. Chen, W.-Y. Hsu, C.-H. Peng, P.-Y. Huang, and P.-C. Peng, "Advanced sensor signal processing for resolving overlapping temperature events in industrial applications," *IEEE Sensors Journal*, 2026.

[16] D. Holler, R. Vaghetto, and Y. Hassan, "Water temperature measurements with a Rayleigh backscatter distributed sensor," *Optical Fiber Technology*, vol. 55, p. 102160, 2020. [Online]. Available: https://linkinghub.elsevier.com/retrieve/pii/S1068520019304559

[17] K. Susanto, J.-P. Malet, X. Chavanne, V. Marc, and J. Gance, "Passively heated fiber optic distributed temperature sensing for long-term soil moisture observations," *Frontiers in Water*, vol. 7, p. 1574618, 2025.

[18] R. Wang, H. Li, C. Liu, J. Dai, C. Cheng, W. Hu, and M. Yang, "Review of fiber optic sensing technologies for leak detection in hydrogen energy storage and transport equipment," *IEEE Sensors Reviews*, vol. 3, pp. 219–242, 2026.

[19] V. F. Bense, T. Read, O. Bour, T. Le Borgne, T. Coleman, S. Krause, A. Chalari, M. Mondanos, F. Ciocca, and J. S. Selker, "Distributed Temperature Sensing as a downhole tool in hydrogeology: SUBSURFACE DTS," *Water Resources Research*, vol. 52, no. 12, pp. 9259–9273, 2016. [Online]. Available: http://doi.wiley.com/10.1002/2016WR018869

[20] L. C. Silva, M. E. Segatto, and C. E. Castellani, "Raman scattering-based distributed temperature sensors: A comprehensive literature review over the past 37 years and towards new avenues," *Optical Fiber Technology*, vol. 74, p. 103091, 2022.

[21] M. B. Hausner, F. Suárez, K. E. Glander, N. v. d. Giesen, J. S. Selker, and S. W. Tyler, "Calibrating Single-Ended Fiber-Optic Raman Spectra Distributed Temperature Sensing Data," *Sensors*, vol. 11, p. 10859, 2011. [Online]. Available: http://www.mdpi.com/1424-8220/11/11/10859

[22] L. Zeni, L. Picarelli, B. Avolio, A. Coscetta, R. Papa, G. Zeni, C. Di Maio, R. Vassallo, and A. Minardo, "Brillouin optical time-domain analysis for geotechnical monitoring," *Journal of Rock Mechanics and Geotechnical Engineering*, vol. 7, no. 4, pp. 458–462, 2015.

[23] M. Iten and A. M. Puzrin, "Botda road-embedded strain sensing system for landslide boundary localization," in *Smart Sensor Phenomena, Technology, Networks, and Systems 2009*, vol. 7293. SPIE, 2009, pp. 333–344.

[24] Bakx, Doornenbal, Weesep, Bense, Essink, and Bierkens, "Determining the Relation between Groundwater Flow Velocities and Measured Temperature Differences Using Active Heating-Distributed Temperature Sensing," *Water*, vol. 11, no. 8, p. 1619, 2019. [Online]. Available: https://www.mdpi.com/2073-4441/11/8/1619

[25] P. Mogensen, "Fluid to duct wall heat transfer in duct system heat storages," *Document-Swedish Council for Building Research*, no. 16, pp. 652–657, 1983.

[26] H. He, M. F. Dyck, R. Horton, T. Ren, K. L. Bristow, J. Lv, and B. Si, "Development and application of the heat pulse method for soil physical measurements," *Reviews of Geophysics*, vol. 56, no. 4, pp. 567–620, 2018.

[27] N. Simon, O. Bour, M. Faucheux, N. Lavenant, H. Le Lay, O. Fovet, Z. Thomas, and L. Longuevergne, "Combining passive and active distributed temperature sensing measurements to locate and quantify groundwater discharge variability into a headwater stream," *Hydrology and Earth System Sciences*, vol. 26, no. 5, pp. 1459–1479, 2022. [Online]. Available: https://hess.copernicus.org/articles/26/1459/2022/

[28] N. Simon and O. Bour, "An Toolbox for Automatically Interpreting Active Distributed Temperature Sensing Measurements," *Groundwater*, p. 13172, 2022. [Online]. Available: https://onlinelibrary.wiley.com/doi/10.1111/gwat.13172

[29] D. Rautenberg, T. Renner, T. Trick, and J. Kriegseis, "Determination of flow velocities using fiber-optic temperature measurements," *Experiments in Fluids*, vol. 65, no. 2, p. 22, 2024.

[30] A. Folch, L. del Val, L. Luquot, L. Martínez-Pérez, F. Bellmunt, H. Le Lay, V. Rodellas, N. Ferrer, A. Palacios, S. Fernández *et al.*, "Combining fiber optic dts, cross-hole ert and time-lapse induction logging to characterize and monitor a coastal aquifer," *Journal of Hydrology*, vol. 588, p. 125050, 2020.

[31] J. S. Selker, L. Thévenaz, H. Huwald, A. Mallet, W. Luxemburg, N. van de Giesen, M. Stejskal, J. Zeman, M. Westhoff, and M. B. Parlange, "Distributed fiber-optic temperature sensing for hydrologic systems," *Water Resources Research*, vol. 42, no. 12, 2006.

[32] S. Schomburgk, D. Jauffret, and T. Pointet, "Etude des nappes aquifères au voisinage du doubs navigable et de ses dérivations entre la limite est du département du doubs et la confluence avec la saône.(no. rp-451463-fr)," BRGM, Tech. Rep., 2002.

[33] J. A. Cherry and R. A. Freeze, *Groundwater*. Englewood Cliffs, NJ: Prentice-Hall, 1979.

[34] M. Romanet, A. Matic, M. Zerbib, K. Huy, J. Labbe, H. Celle, and J.-C. Beugnot, "Distributed brillouin optical fiber temperature sensor for groundwater flow measurement," in *Proceedings of SPIE*, vol. 12643, 2023.

[35] M. Merklein, I. V. Kabakova, A. Zarifi, and B. J. Eggleton, "100 years of Brillouin scattering: Historical and future perspectives," *Applied Physics Reviews*, vol. 9, no. 4, 2022.

[36] C. Sayde, C. K. Thomas, J. Wagner, and J. Selker, "High-resolution wind speed measurements using actively heated fiber optics," *Geophysical Research Letters*, vol. 42, no. 22, pp. 10–064, 2015.

[37] M. Vélez Márquez, J. Raymond, D. Blessent, M. Philippe, N. Simon, O. Bour, and L. Lamarche, "Distributed Thermal Response Tests Using a Heating Cable and Fiber Optic Temperature Sensing," *Energies*, vol. 11, no. 11, p. 3059, 2018. [Online]. Available: http://www.mdpi.com/1996-1073/11/11/3059

[38] N. Simon, O. Bour, N. Lavenant, G. Porel, B. Nauleau, B. Pouladi, L. Longuevergne, and A. Crave, "Numerical and experimental validation of the applicability of active-dts experiments to estimate thermal conductivity and groundwater flux in porous media," *Water Resources Research*, vol. 57, no. 1, p. e2020WR028078, 2021.

[39] J. Raymond and L. Lamarche, "Development and numerical validation of a novel thermal response test with a low power source," *Geothermics*, vol. 51, pp. 434–444, 2014.

[40] J. Labbe, M. Romanet, H. Celle, M. Zerbib, K. P. Huy, A. Matic, V. Klaba, G. Mailhot, and J.-C. Beugnot, "A new approach for groundwater fluxes assessment in alluvial aquifers using active-dts with a Brillouin-based sensor," *Journal of Hydrology*, p. 135336, 2026.

[41] F. Stauffer, P. Bayer, P. Blum, N. Molina-Giraldo, and W. Kilzenbach, "Thermal use of shallow subsurface," 2013.

[42] F. Fossoul, P. Orban, and A. Dassargues, "Numerical simulation of heat transfer associated with low enthalpy geothermal pumping in an alluvial aquifer," *Geologica belgica*, vol. 14, no. 1-2, 2011.

[43] S. Wildemeersch, P. Jamin, P. Orban, T. Hermans, M. Klepikova, F. Nguyen, S. Brouyère, and A. Dassargues, "Coupling heat and chemical tracer experiments for estimating heat transfer parameters in shallow alluvial aquifers," *Journal of Contaminant hydrology*, vol. 169, pp. 90–99, 2014.

[44] J. L. Schaper, C. Zarfl, K. Meinikmann, E. W. Banks, S. Baron, O. A. Cirpka, and J. Lewandowski, "Spatial variability of radon production rates in an alluvial aquifer affects travel time estimates of groundwater originating from a losing stream," *Water Resources Research*, vol. 58, no. 4, p. e2021WR030635, 2022.

[45] Y. Mizuno, N. Hayashi, H. Fukuda, K. Y. Song, and K. Nakamura, "Ultrahigh-speed distributed brillouin reflectometry," *Light: Science & Applications*, vol. 5, no. 12, pp. e16 184–e16 184, 2016.

[46] H. Zhang, D. Zhou, B. Wang, C. Pang, P. Xu, T. Jiang, D. Ba, H. Li, and Y. Dong, "Recent progress in fast distributed brillouin optical fiber sensing," *Applied Sciences*, vol. 8, no. 10, p. 1820, 2018.

[47] S. Colombel, M. Romanet, P. Sillard, G. Labroille, L. Andreoli, K. H. Tow, and J.-C. Beugnot, "Distributed brillouin measurement in graded index multimode optical fiber," in *Optical fiber sensor*, 2025.